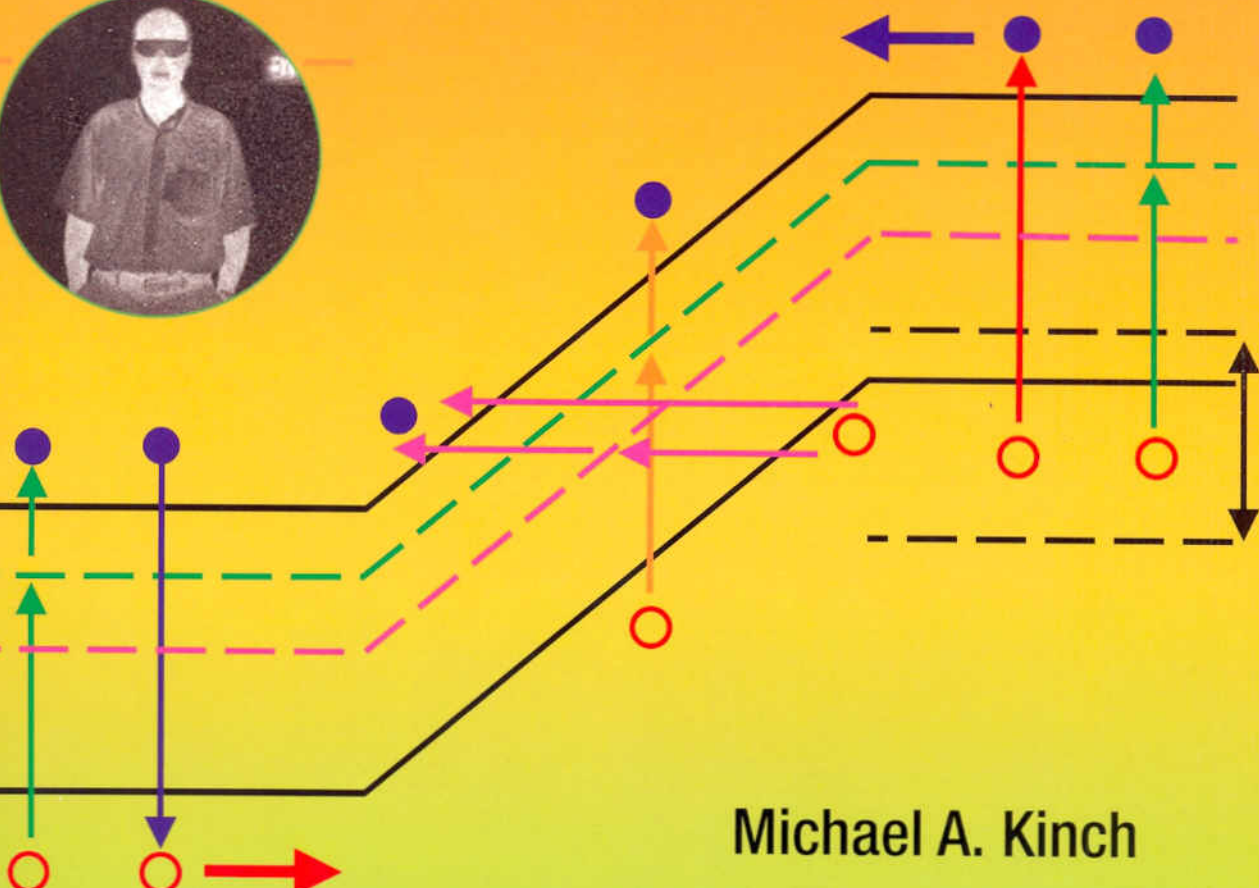




FUNDAMENTALS OF

Infrared Detector Materials



Michael A. Kinch

FUNDAMENTALS OF

Infrared Detector Materials

Michael A. Kinch

Tutorial Texts in Optical Engineering
Volume TT76

SPIE
PRESS

Bellingham, Washington USA

Contents

1	Introduction	1
2	IR Detector Performance Criteria	5
2.1	Photon Detectors	5
2.1.1	IR detector operating temperature	5
2.1.2	IR detector sensitivity	7
2.2	Thermal Detectors	9
3	IR Detector Materials: A Technology Comparison	13
3.1	Intrinsic Direct Bandgap Semiconductor	13
3.2	Extrinsic Semiconductor	16
3.3	Quantum Well IR Photodetectors (QWIPs)	18
3.4	Silicon Schottky Barrier Detectors	23
3.5	High-Temperature Superconductor	26
3.6	Conclusions	27
4	Intrinsic Direct Bandgap Semiconductors	31
4.1	Minority Carrier Lifetime	32
4.1.1	Radiative recombination	32
4.1.2	Auger recombination	33
4.1.3	Shockley–Read recombination	34
4.2	Diode Dark Current Models	34
4.3	Binary Compounds	35
4.3.1	Indium antimonide: InSb	35
4.4	Ternary Alloys	37
4.4.1	Mercury cadmium telluride: $Hg_{1-x}Cd_xTe$	37
4.5	$Pb_{1-x}Sn_xTe$	42
4.5.1	Minority carrier lifetime	43
4.5.2	Dark currents	44
4.6	Type III Superlattices	45
4.6.1	Superlattice bandstructure	45
4.6.2	Band offsets and strain	47
4.6.3	Interdiffusion in HgTe/CdTe superlattices	48
4.6.4	Misfit dislocations	48
4.6.5	Absorption coefficient	49

4.6.6	Effective mass	51
4.6.7	Minority carrier lifetime	52
4.7	Type II Superlattices	53
4.7.1	Minority carrier lifetime	54
4.8	Direct Bandgap Materials: Conclusions	57
4.8.1	HgCdTe	57
4.8.2	InSb	57
4.8.3	PbSnTe	58
4.8.4	Type III superlattices	59
4.8.5	Type II superlattices	59
4.8.6	Final thoughts	59
5	HgCdTe: Material of Choice for Tactical Systems	61
5.1	HgCdTe Material Properties	61
5.1.1	Material growth	61
5.1.2	HgCdTe annealing	65
5.1.3	HgCdTe properties	67
5.2	HgCdTe Device Architectures	75
5.2.1	DLHJ architecture	76
5.2.2	Bump-bonded ion implant architecture	77
5.2.3	Vertically integrated photodiode (VIP and HDVIP) architectures	77
5.3	ROIC Requirements	81
5.3.1	Detector performance: Modeling	82
5.3.2	Dark current in HgCdTe diodes	82
5.3.3	1/f noise	87
5.4	Detector Performance	89
5.5	HgCdTe: Conclusions	91
6	Uncooled Detection	93
6.1	Thermal Detection	93
6.2	Photon Detection	95
6.2.1	HOT detector theory	95
6.2.2	HOT detector data	101
6.2.3	HOT detector contacts	103
6.2.4	HOT detector options	103
6.3	Uncooled Photon vs. Thermal Detection Limits	105
6.4	Uncooled Detection: Conclusions	107
7	HgCdTe Electron Avalanche Photodiodes (EAPDs)	109
7.1	McIntyre's Avalanche Photodiode Model	110
7.2	Physics of HgCdTe EAPDs	112
7.2.1	High-energy scattering rates	113
7.2.2	Electron impact ionization rate in HgCdTe	115

7.3 Empirical Model for Electron Avalanche Gain in HgCdTe	121
7.4 Room-Temperature HgCdTe APD Performance	129
7.5 Monte Carlo Modeling	131
7.6 Conclusions	133
8 Future HgCdTe Developments	135
8.1 Dark Current Model	135
8.1.1 N-side	136
8.1.2 P-side	137
8.2 The Separate Absorption and Detection Diode Structure	139
8.3 Multicolor and Multispectral FPAs	141
8.4 High-Density FPAs	143
8.5 Low Background Operation	143
8.5.1 LWIR 14 μm at 40 K	143
8.5.2 Low background operation at a cutoff of 25 μm	144
8.6 Higher Operating Temperatures	145
8.6.1 High-gain APDs	147
8.7 Conclusion	148
Epilogue	149
Appendix A: Mathcad Program for HgCdTe Diode Dark Current Modeling	151
References	165
About the Author	169
Index	171

Index

- absorption coefficient, 49–51
absorption quantum efficiency, 7
 α -silicon thermal detector
 technologies, 11
annealing, 65–66
antenna structures, 22
APD. *See* avalanche photodiodes.
Auger lifetime, 155–163
Auger minority carrier lifetime properties, 73–74
Auger recombination, 33–34
Auger transitions, 56
Avalanche photodiodes (APDs), 109
 high-gain, 147–148
 theory, 109

Background limited performance (BLIP), 6, 93, 143
band offsets and strain, 47–48
band structure, 67
bandgap engineering, 19
bandgap materials, direct, 57
bandgap states, tunneling via, 84–85
binary compounds, 35–37
 indium antimonide, 35–37
BLIP. *See* background limited performance.
bump-bonded ion implant architecture, 77

coefficient of thermal expansion (CTE), 74–75
CTE. *See* coefficient of thermal expansion.
cutoff wavelengths, 144–145

dark current
 HgCdTe diodes and, 82–86
Mathcad program modeling, 151–163
Auger lifetime, 155–163
minority carrier lifetime modeling, 153–154
n-type, 153
p-type, 152–153
model
 diffusion current, 136
 infrared devices and future development of, 135–139
 N-side, 136–137
 P-side, 137–139
 PbSnTe direct bandgap alloy and, 43–44
 total, 85–86
dead voltage model, 121–125
depletion current, 84
detector contacts, HOT theory and, 103
detector data, HOT theory and, 101–103
detector performance, 82
diffusion current, 83, 136, 137
diode dark current models, 34–35
direct bandgap materials, 57–59
 HgCdTe, 57
 InSb, 57–58
 PbSnTe, 58–59
superlattices
 type II, 59
 type III, 59
direct tunneling, 85
dislocation density, 74–75
DLHJ diodes. *See* double layer heterojunction diodes.
doping, *p*-type mercury cadmium telluride and, 40–41

- double layer heterojunction diodes
 (DLHJ), 38
 architecture, 76–77
- double-layer p⁺/n heterojunctions. *See*
 double layer heterojunction diodes.
- DRS manufacturing, 89–91
 HDVIP technologies, 89
 VIP technologies, 89
- EAPDs. *See* electron avalanche photodiodes
- effective mass, 51–52
- electron avalanche photodiodes, 109
- electron impact ionization rate, 115–120
 Kronig–Penney model, 118
- electron transport, HgCdTe and, 69–70
- extrinsic semiconductor, 16–18
- extrinsically doped *p*-type mercury cadmium telluride, 40
- Focal plane array (FPA), 2
 high density, 143
 multicolor, 141–143
 multispectral, 141–143
- FPA. *See* focal plane array.
- Glow discharge mass spectroscopy, 63
- HDVIPTM architecture, 77–81
 liquid phase epitaxial material growth, 79
 technologies, 89
- HgCdTe annealing, 65–66
- HgCdTe avalanche photodiodes, room-temperature, 129–131
- HgCdTe device architecture, 75–81
 bump-bonded ion implant, 77
 DLHJ, 76–77
 vertically integrated photodiode, 77–81
- HgCdTe diode dark current, Mathcad program modeling, 151–163
 Auger lifetime, 155–163
 minority carrier lifetime modeling, 153–154
 n-type, 153
 p-type, 152–153
- HgCdTe diodes, dark current and, 82–86
- sources of,
 depletion current, 84
 diffusion current, 83
 surface generation current, 84
 total dark current, 85–86
 tunneling, 84–85
- HgCdTe electron avalanche photodiodes (EAPDs), 109–137
 APD theory, 109
 empirical model for, 121–129
 dead voltage model, 121–125
 McIntyre's model, 110–112
 Monte Carlo modeling, 131–133
 physics of, 112–120
 electron impact ionization rate, 115–120
 high energy scattering rates, 113–115
- HgCdTe materials, 61–91
 detector performance, 89–91
 glow discharge mass spectroscopy, 63
 growth of, 61–65
 Liquid phase epitaxy (LPE), 61, 62–64
 Metal–organic chemical vapor deposition (MOCVD), 61, 65
 Metal–organic vapor phase epitaxy (MOVPE), 65
 Molecular beam epitaxy (MBE), 61, 64–65
 physical properties, 74–75
 coefficient of thermal expansion, 74–75
 dislocation density, 74–75
 lattice constant, 74
 properties of, 61–75
 band structure, 67
 minority carrier lifetime properties, 73–74
 Auger, 73–74
 radiative, 73–74
 Shockley–Read, 73–74
 optical properties, 67
 transport, 67–73
 electron transport, 69–70
 hole transport, 71–73
- ROIC requirements, 81–89

- HgTe/CdTe superlattices, 48
interdiffusion, 48
high density FPA, 143
high energy scattering rates, 113–115
high gain APDs, 147–148
High operating temperature (HOT) photon detection, 95–101
detector contacts, 103
detector data, 101–103
options, 103–105
high temperature operations, infrared devices and, 145–148
high-gain APDs, 147–148
High temperature superconductor (HTC), 26–27
hole transport, HgCdTe and, 71–73
HOT. *See* high operating temperature.
HTC. *See* high temperature superconductor.
- impact ionization rate, 115–120
Indium antimonide (InSb), 35–37
IR detection material, 57–58
Infrared (IR) detectors, 1–3
absorption quantum efficiency, 7
DRS manufacturing, 89–91
early types, 1
first generation models, 1
focal plane array (FPA), 2
future development of, 135–148
dark current model, 135–139
high-density FPA, 143
higher operating temperatures, 145–148
low background operation, 143
multicolor FPA, 141–143
multispectral FPA, 141–143
separate absorption and detection structure, 139–141
required properties, 135
future models, 2
performance criteria, 5–11, 89–91
photon type, 5–9, 13–29
scanning arrays, 2
second generation models, 1–2
sensitivity of, 7–9
noise equivalent irradiance, 7
signal flux, 7
thermal detectors, 9–11
time, delay and integrate (TDI)
techniques, 2
InSb. *See* indium antimonide.
interdiffusion, HgTe/CeTe superlattices and, 48
intrinsic direct bandgap semiconductor, 13–16, 27, 31–59
binary compounds, 35–37
diode dark current models, 34–35
materials, HgCdTe, 57
InSb, 57–58
PbSnTe, 58–59
type II superlattices, 59
minority carrier lifetime, 32–34
PbSnTe, 42–44
ternary alloys, 37–42
type II superlattices, 53–57
type III superlattices, 45–53, 59
IR. *See* infrared.
ionization rate, 115–120
- Kronig–Penney model, 118
- lattice constant, 74
Liquid phase epitaxy (LPE), 61, 62–64, 79
low background operation, 143
LWIR 14 μm at 40 K, 143–144
25 μm cutoff wavelength, 144–145
LPE. *See* liquid phase epitaxy.
LWIR
14 μm at 40 K, 143–144
minority carrier lifetimes and, 56
spectral bands, 37
- majority carrier, 5–7
detection, photoconductive, 5
Mathcad programming modeling for dark current, 151–163
MBE. *See* molecular beam epitaxy.
McIntyre's avalanche photodiode model, 110–112
mercury cadmium telluride, 37–41
double layer heterojunction
diodes, 38
LWIR spectral bands, 37

- mercury cadmium telluride (*Continued*)
 MWIR spectral bands, 37
n-type, 37–39
p-type, 39–41
- Metal organic chemical vapor deposition (MOCVD), 61
- Metal organic vapor phase epitaxy (MOVPE), 65
- microlenses, 22
- minority carrier devices, 5–7
 detection, responsivity and noise, 5
 lifetime, 32–34
 Auger
 recombination, 33–34
 transitions, 56
- LWIR, 56
- MWIR, 56
- PbSnTe direct bandgap alloy and, 43–44
- properties
 Auger, 73–74
 HgCdTe and, 73–74
 radiative, 73–74
 Shockley–Read, 73–74
 radiative recombination, 32–33
 Shockley–Read recombination, 34
 type II superlattices and, 54–57
 type III superlattices and, 52–53
- misfit dislocations, 48–49
- MOCVD. *See* metal organic chemical vapor deposition.
- MOVPE. *See* metal organic vapor phase epitaxy.
 modeling, Mathcad program for dark current, 151–163
- Molecular beam epitaxy (MBE), 61, 64–65
- Monte Carlo modeling, 131–133
- multicolor FPA, 141–143
- multippectral FPA, 141–143
- MWIR
 minority carrier lifetimes and, 56
 spectral bands, 37
- Noise equivalent irradiance (NEI), 7
- Noise equivalent temperature ($\text{NE}\Delta T$), 9
- noise, minority carrier detection and, 5
- N-side, dark current model and, 136–137
- N type
 dark current Mathcad program
 modeling, 153
 mercury cadmium telluride and, 37–39
1/f noise, 87–89
- operating temperatures, infrared devices and, 145–148
- optical properties, 67
- P type dark current Mathcad program
 modeling, 152–153
- PbSnTe direct bandgap alloy, 42–44
 dark currents, 44
 as IR detection material, 58–59
 minority carrier lifetime, 43–44
- photon conductive detection, 5
- photon detectors, 5–9, 95–105
 background limited performance, 6
 extrinsic semiconductor, 16–18
 high temperature superconductor, 26–27
 HOT theory, 95–101
 detector
 contacts, 103
 data, 101–103
- intrinsic direct bandgap semiconductor, 13–16
- majority carrier, 5–7
- minority carrier, 5–7
- quantum well types, 18–23
- silicon Schottky barrier type, 23–25
- thermal generation rate, 6–7
- photon uncooled detection vs. thermal detection limits, 105–107
- P-side, dark current model and, 137–139
- p*-type mercury cadmium telluride, 39–41
 extrinsically doped *p*-type, 40
 general doping, 40–41
 vacancy-doped *p*-type, 39–40
- Quantum well IR photodetectors (QWIPs), 18–23
- bandgap engineering, 19
- NEI. *See* noise equivalent irradiance.
- $\text{NE}\Delta T$. *See* noise equivalent temperature.

- superlattice, 18
thermal generation rate, 22
- QWIPs.* *See quantum well IR photodetectors.*
- radiative lifetime, 153–154
radiative minority carrier lifetime properties, 73–74
radiative recombination, 32–33
resonant structures, 22
responsivity, minority carrier detection and, 5
ROIC requirements, 81–89
 detector performance, 82
 HgCdTe diodes, 82–86
 1/f noise, 87–89
room-temperature HgCdTe APD performance, 129–131
- SAD. *See separate absorption and detection.*
- SB. *See Schottky barriers.*
- scanning arrays, 2
- Shockley–Read minority carrier lifetime properties, 73–74
- Schottky barriers (SB), 23–25
- semiconductors
 extrinsic, 16–18
 intrinsic direct bandgap, 13–16, 31–59
 PbSnTe bandgap alloy, 42–44
- separate absorption and detection (SAD) structure, 139–141
- Shockley–Read recombination, 34
- signal flux, 7
- Silicon Schottky barrier (SB) detectors, 23–25
- superlattices
 bandstructure, 45–47
 HgTe/CdTe, 48
 type II, 53–57, 59
 type III, 45–53, 59
 types, 18–19
- surface generation current, 84
- TDI. *See time, delay and integrate.*
- ternary alloys, 37–42
- ternary alloys, mercury cadmium telluride, 37–41
- thermal detection, 93–95
 limits vs. photon uncooled detection, 105–107
- thermal detectors, 9–11
 noise equivalent temperature, 9
- technologies
 α -silicon, 11
 thin-film ferroelectrics, 11
 vanadium oxide, 11
- thermal generation rate, 6–7, 22
 antenna structures, 22
 microlenses, 22
 resonant structures, 22
- thin film ferroelectrics, 11
- Time, delay and integrate (TDI)
 techniques, 2
- total dark current, 85–86
- transport properties, HgCdTe and, 67–73
- tunneling via bandgap states, 84–85
- tunneling, direct, 85
- type II superlattices, 53–57, 59
 minority carrier lifetime, 54–57
 Auger transitions, 56
- type III superlattices, 45–53, 59
 absorption coefficient, 49–51
 band offsets and strain, 47–48
 bandstructure, 45–47
 effective mass, 51–52
 HgTe/CdTe, 48
 minority carrier lifetime, 52–53
 misfit dislocations, 48–49
- uncooled detection, 93–107
 BLIP performance, 93
 photon, 95–105
 thermal detection limits vs., 105–107
- thermal, 93–95
- vacancy-doped *p*-type mercury cadmium telluride, 39–40
- vanadium oxide thermal detector technologies, 11
- vertically integrated photodiode (VIP), 77–81, 89
- VIP. *See vertically integrated photodiode.*